A Computational Approach for Generalized Equal Width Wave Equation Using Cubic Trigonometric B-Spline Differential Quadrature Method

Arshed Ali[1], Aiman Hayat[1], Imtiaz Ahmad[2], Hadia Atta[1]
[1]Department of Mathematics, Islamia College Peshawar, Pakistan.
[2]Institute of Informatics and Computing in Energy (IICE), University Tenaga Nasional (UNITEN), Kajang, Selangor, Malaysia
*Correspondence: arshad.ali@icp.edu.pk

Citation | Ali. A, Hayat. A, Ahmad. I, Atta. H, "A Computational Approach for Generalized Equal Width Wave Equation Using Cubic Trigonometric B-Spline Differential Quadrature Method", IJIST, Vol. 8 Issue.3 pp1408-1428, June2026
DOI: https://doi.org/10.33411/IJIST/1934
Received | May 09, 2026 **Revised |** June11, 2026 **Accepted |** June15, 2026 **Published |** June24, 2026.

In this paper, a computational method of solving the generalized equal width (GEW) wave equation is proposed, which describes high-order nonlinear shallow water waves. The proposed approach uses cubic trigonometric B-spline (CTBS) basis functions for spatial discretization, together with the classical fourth-order Runge-Kutta scheme for time integration, and the differential quadrature method (DQM) for spatial approximation. This approach leads to the derivation of a set of ordinary differential equations (ODEs) for the CTBS-DQM system, followed by efficient solution of the system with the ODE solver. Numerical experiments are performed for the propagation of a single solitary wave and interaction between two positive solitary waves with different nonlinearity orders (p = 2, 3, 4) and amplitudes, respectively. Error norms (L_2andL_∞) and conservation invariants (C_1, C_2, C_3) are used to evaluate the accuracy and reliability of the proposed scheme. The present method achieves exceptionally small errors, with $L_\infty = 1.14 \times 10^{-5}$ and $L_2 = 1.77 \times 10^{-5}$ for $p = 2$ at $t = 20$, and demonstrates a convergence rate of approximately **4. 04**. A comparative analysis of the present CTBS-DQM with existing cubic B-spline Galerkin and quintic B-spline DQM methods shows that the present approach gives superior results in terms of accuracy with much lesser computational cost, achieving a 97.6% reduction in CPU time (from 297.13 seconds to 7.23 seconds) while maintaining similar or better accuracy levels. The efficiency of the proposed approach is further validated through convergence analysis, and by comparing CPU time, thereby establishing the proposed method as a useful tool for the simulation of the high-order nonlinear wave phenomena.

Keywords: Generalized Equal Width Wave Equation**,** Cubic Trigonometric B-Splines**,** Differential quadrature method, Solitary Wave Interaction, Nonlinear Shallow Water Waves.

Introduction:

Nonlinear partial differential equations (PDEs) are indispensable tools for modelling a wide range of physical phenomena, including shallow water waves, plasma oscillations, and nonlinear optics. Among these, the family of equal width wave equations **has** received special attention for their capacity to describe long waves traveling in shallow water without losing their solitary wave structure. The generalized equal width (GEW) wave equation extends the classical equal width (EW) and modified equal width (MEW) equations by incorporating a higher-order nonlinear term. It is commonly expressed as

$$\frac{\partial w}{\partial t} + \varepsilon w^p \frac{\partial w}{\partial x} - \mu \frac{\partial^3 w}{\partial t \partial x^2} = 0,$$

where $w = w(x,t)$, ε and μ are positive constants, and p is a positive integer. This equation is closely related **to** both the regularized long wave (RLW) and the Korteweg–de Vries (KdV) equations, both of which are well known for their solitary wave characteristics [1][2]. The standard EW equation is recovered when $p = 1$, whereas setting $p = 2$ yields the MEW equation [3].

Literature Review:

Over the past decades, a variety of numerical methods have been developed to solve the GEW equation for different nonlinearity orders ($p = 2,3,4$), corresponding to cubic, quartic, and quintic nonlinear cases. Early works include Galerkin finite element methods with quadratic and cubic B-splines [4], collocation methods using cubic and septic B-splines[4][5], and Petrov–Galerkin approaches [6]. Evans and Raslan [4] applied a quadratic B-spline collocation method to the GEW equation, while Raslan [5] extended the work using cubic B-splines. [6] employed a Petrov–Galerkin finite element method with quadratic B-spline trial functions.

In the context of B-spline based methods, [7] presented a cubic B-spline Galerkin approach for the GEW equation and computed error norms and invariants for single and interacting solitary waves. Subsequently, [8] developed a septic B-spline collocation method, and [9] applied quintic B-spline collocation. Recently, [10] investigated the GEW equation using a subdomain finite element method with sextic B-splines.

Finite difference methods (FDM) have also been widely used. For example,[11] presented a fully implicit finite difference solution to the GEW equation. Higher-order methods based on the integration of FDM with the differential quadrature method (DQM) have also been used.In particular,[12] proposed a hybrid method based on FDM and quintic B-spline DQM that is efficient in terms of accuracy for single solitary waves and interactions (including two positive, two negative, and mixed amplitude cases) for cubic, quartic and quintic nonlinearities. [13]Useda pseudospectral method with delta-shaped basis functions.

Operator splitting techniques have also been applied. For example,[7] proposed a Lie–Trotter splitting algorithm combined with a cubic B-spline lumped Galerkin method. The splitting decomposed the GEW equation into linear and nonlinear sub-equations, and the resulting numerical scheme was shown to be unconditionally stable.

Outside the GEW equation but relevant to the numerical methodology, several researchers have successfully applied cubic trigonometric B-splines (CTBS) and differential quadrature methods to other classes of PDEs. For instance, [14] developed a CTBS-based computational model for second-order partial integro-differential equations (PIDEs). The article[15] used a differential quadrature approach based on B-splines for Volterra PIDs with weakly singular kernels. More recently, [16] proposed an efficient radial basis function (RBF) collocation approach for fractional PIDEs, and [17] applied DQM with local RBFs to fractional advection-diffusion models. Furthermore, [18] combined fractional Euler methods

with CTBS for time-fractional nonlinear PIDEs. These works demonstrate the versatility and accuracy of CTBS and DQM frameworks.

In recent years, there has been significant progress in the development of advanced numerical methodologies for solving various classes of partial differential equations (PDEs) and fractional differential equations arising in diverse scientific and engineering applications. Meshless methods, particularly those based on radial basis functions (RBFs), have gained considerable attention due to their ability to handle complex geometries and irregular domains without requiring structured meshes [19][20][21][22][23]. [19]Presented a computational study of time-fractional Kawahara equations using quintic B-spline and Galerkin's method. [20]Developed hybrid methodologies combining operator splitting with meshless methods for multi-dimensional fractional PDEs. [22] applied Pascal polynomial numerical approaches to elliptic inverse heat conduction problems, while [16] developed an efficient RBF-based collocation approach for fractional PIDEs.

[24]Proposed a meshless method combined with operator splitting for solving the Allen-Cahn equation. [25]Demonstrated the effectiveness of Hermite wavelet polynomials for solving one-dimensional PDEs using artificial neural networks. [26]Developed physics-informed fractional machine learning frameworks for non-local integro-partial differential equations. [27]Introduced a generalized Haar wavelet-homotopy method for solving differential and partial differential equations. The growing interest in fractional calculus has led to the development of innovative schemes, including physics-informed fractional machine learning frameworks [26] and generalized Haar wavelet-homotopy methods [27] for non-local integro-PDEs.

In the context of spline-based differential quadrature methods, which are most relevant to the present work, several significant advancements have been reported recently. [28]Introduced a modified quintic trigonometric B-spline differential quadrature method (MQTB-DQM) for the improved Boussinesq equation, successfully simulating complex solitary wave behaviors including splitting and multi-soliton interactions. Furthermore, a quintic uniform algebraic trigonometric tension B-spline differential quadrature approach was proposed for the coupled Korteweg-de Vries equation, demonstrating sixth-order accuracy and excellent conservation properties [29]. For nonlinear viscous wave equations, a comparative study of modified cubic B-spline differential quadrature methods (MCB-DQM) revealed that these schemes are unconditionally stable and offer a favorable balance between accuracy and computational cost [30]. Additionally, the numerical solution of the Sine-Gordon equations has been advanced through a new DQM based on cubic unified and extended trigonometric B-spline functions, which exhibits second-order convergence in space [31]. These recent advances in numerical analysis provide a solid foundation for the development of robust, efficient, and accurate computational frameworks, such as the CTBS-DQM approach proposed in this work, for solving challenging nonlinear wave equations with high-order

Motivation and Objectives:

Despite the progress, several challenges remain.The existing approaches to the GEW equation are often expensive because they require high-order B-splines or dense matrices or lack the accuracy to account for high-order nonlinear terms and complex wave interactions (e.g., two negative amplitudes or mixed signs).Furthermore, the DQM framework has not been investigated yet for the GEW equation using cubic trigonometric B-splines.Trigonometric B-splines have features that make them superior to polynomial B-splines: they naturally accommodate periodic or Dirichlet boundary conditions, they result in narrower bandwidth matrices (generally tridiagonal or pentadiagonal), and they have high approximation order for a small number of grid points.

To overcome this limitation, this work introduces a numerical scheme for solving the GEW equation, which combines cubic trigonometric B-spline basis functions for spatial approximation with the standard fourth-order Runge–Kutta technique for time stepping referred to as the CTBS-RK4 method. The main benefits of this proposed approach include:
The CTBS functions yield a tridiagonal system, significantly reducing computational overhead compared to global methods.
DQM provides high-order accuracy in space with relatively coarse grids.
The time integration scheme is explicit, stable, and easy to implement.
Comprehensive numerical experiments are carried out for:
Single solitary wave propagation for $p = 2,3,4$ with both large and small amplitudes.

Interaction of two solitary waves for three scenarios: two positive amplitudes. These interactions are examined for cubic $(p = 2)$, quartic $(p = 3)$ and quintic $(p = 4)$ nonlinearities.

The effectiveness of the proposed technique is verified with error norms $L_2$and L_∞, conservation invariants (I_1, I_2, I_3) (mass, momentum, energy), convergence rate and CPU time.However, the results of this CTBS-DQM scheme are compared with that of existing cubic B-spline Galerkin[32] and quintic B spline DQM [12] schemes and the present scheme outperforms them with much less computational time.

The proposed CTBS-DQM method has significant practical applications across various scientific and engineering fields, including shallow water wave modeling (tsunamis, tidal waves, storm surges), fluid dynamics (wave propagation in channels, river flows, ocean currents), plasma physics (ion-acoustic waves and soliton interactions), nonlinear optics (pulse propagation in optical fibers), environmental engineering (coastal structure interaction, sediment transport), renewable energy (wave energy converter design), and geophysical fluid dynamics. The method's ability to accurately simulate high-order nonlinear wave phenomena with high computational efficiency makes it a valuable tool for these diverse applications.

Novelty of the Study:

The novelty of the present work lies in the following key aspects:

First Application of CTBS-DQM to GEW Equation:

This is the first study to apply cubic trigonometric B-splines combined with the differential quadrature method for solving the generalized equal width equation. While polynomial B-splines have been used extensively, trigonometric B-splines have not been explored for the GEW equation.

Superior Computational Efficiency:

The CTBS basis functions yield a tridiagonal system, dramatically reducing computational overhead compared to global methods. The proposed scheme achieves a 97.6% reduction in CPU time compared to the quintic B-spline DQM method [12] while maintaining similar or better accuracy.

High Accuracy with Coarse Grids:

The CTBS-DQM approach provides fourth-order convergence in space, allowing accurate solutions with significantly fewer grid points than existing methods.

Robustness for High-Order Nonlinearities:

The method successfully handles high-order nonlinearities $(p = 3,4)$ and complex wave interactions without spurious oscillations, demonstrating stability and accuracy for strongly nonlinear problems.

Natural Handling of Boundary Conditions:

The modified CTBS basis functions naturally incorporate Dirichlet boundary conditions, simplifying implementation and improving accuracy near boundaries.

These features distinguish the CTBS-DQM method from existing approaches such as polynomial B-spline Galerkin methods [32], septic B-spline collocation [8], and quintic B-spline DQM [12] which either require denser grids, higher-order splines, or exhibit larger numerical errors.

Outline of the Paper:

The structure of this paper is as follows. Section 2 describes the CTBS-DQM spatial discretization, the semi-discrete formulation, and the fourth-order Runge–Kutta time integration. Section 3 presents the numerical results, including tables and figures for single solitary waves and interacting waves. Also, provides a discussion of the results, convergence analysis, and CPU time comparisons. Lastly, Section 4 summarizes the main conclusions drawn from this work and proposes potential avenues for further investigation.

Methodology:

Problem Statement:

We examine the generalized equal width wave equation expressed as

$$\frac{\partial w}{\partial t} + \varepsilon w^p \frac{\partial w}{\partial x} - \mu \frac{\partial^3 w}{\partial t \partial x^2} = 0, \quad t > 0, \quad a \le x \le b \qquad (1)$$

Accompanied by the initial condition

$$w(x,0) = \gamma_0(x), \ (2)$$

And the boundary conditions

$$w(a,t) = \gamma_1(t), \ w(b,t) = \gamma_2(t), \ t \ge 0. \ (3)$$

where p is a positive integer representing the nonlinearity order ($p = 2,3,4$ for cubic, quartic, and quintic nonlinearities, respectively). This formulation accommodates the classical equal width equation ($p = 1$), the modified equal width equation ($p = 2$), and higher-order nonlinearities ($p = 3,4$). In this system, $w = w(x,t)$ denotes the dependent variable to be determined, while ε and μ are fixed positive parameters. The independent quantities t and x correspond to spatial position and elapsed time, respectively. The functions $\gamma_0, \gamma_1, \gamma_2$ are assumed to be sufficiently regular (smooth) and are prescribed a priori.

Discretization with CTBS-DQM:

Let the spatial domain $[a,b]$ be divided into $N+1$ equally spaced nodes

$$x_m = a + mh, \ \ m = 0,1,\dots,N, \qquad h = (b-a)/N$$

The time interval $[0,T]$ is discretized as $t_k = k\Delta t, k = 0,1,\dots,L$ with time step Δt.

Cubic Trigonometric B-Splines:

The CTBSfunctions $J_m(x)$, are defined piecewise as

$$J_m(x) = \frac{1}{\vartheta}\begin{cases} \rho_{m-2}^3, & x_{m-2} \le x < x_{m-1}, \\ \rho_{m-2}(\rho_{m-2}q_m + q_{m+1}\rho_{m-1}) + q_{m+1}\rho_{m-1}^2, & x_{m-1} \le x < x_m, \\ \rho_{m-2}q_{m+1}^2 + q_{m+2}(\rho_{m-1}q_{m+1} + q_{m+2}\rho_m), & x_m \le x < x_{m+1}, \\ q_{m+2}^3, & x_{m+1} \le x < x_{m+2}, \\ 0, & \text{othwerwise}, \end{cases}$$

where $\theta = \sin\left(\frac{h}{2}\right)\sin(h)\sin\left(\frac{3h}{2}\right)$, $\rho_m = \sin\left(\frac{x-x_m}{2}\right)$, $q_m = \sin\left(\frac{x_m-x}{2}\right)$.

The set $J_m(x)$, $m = -1\dots N+1$, forms a basis over $[a,b]$. The values of J_m and its derivatives at the knots are given in Lemma 1.

Lemma 1: The function values and derivatives at the node x_n are:

$$J_m(x_n) = \begin{cases} \beta_2, & \text{if } m = n, \\ \beta_1, & \text{if } m = n+1 \text{ or } m = n-1, \\ 0, & \text{otherwise}, \end{cases}$$

$$J'_m(x_n) = \begin{cases} \beta_4, & \text{if } m = n+1, \\ \beta_3, & \text{if } m = n-1, \\ 0, & \text{otherwise}, \end{cases}$$

and

$$J''_m(x_n) = \begin{cases} \beta_6, & \text{if } m = n, \\ \beta_5, & \text{if } m = n+1 \text{ or } m = n-1, \\ 0, & \text{otherwise}, \end{cases}$$

where

$$\beta_1 = \frac{\sin^2\left(\frac{h}{2}\right)}{\sin(h)\,\sin\left(\frac{3h}{2}\right)}, \beta_2 = \frac{2}{1+\cos(h)}, \beta_3 = -\frac{3}{4\sin\left(\frac{3h}{2}\right)}, \beta_4 = \frac{3}{4\sin\left(\frac{3h}{2}\right)},$$

$$\beta_5 = \frac{3(1+3\cos(h))}{16\sin^2\left(\frac{h}{2}\right)\left(2\cos\left(\frac{h}{2}\right)+\cos\left(\frac{3h}{2}\right)\right)}, \beta_6 = \frac{-3\cot^2\left(\frac{h}{2}\right)}{2+4\cos(h)}.$$

Differential Quadrature (DQ) Approximation:

In the DQ method, the k-th order spatial derivative at node x_r) is approximated by a weighted sum of the function values at all nodes:

$$\frac{\partial^k w(x_r,t)}{\partial x^k} = \sum_{l=1}^{N} a_{rl}^k\, w(x_l,t), \qquad r \in I_1 = \{1,2,\dots,N\},$$

where$a_{rl}^{(k)}$ are the weighting coefficients.

To determine these coefficients, we use a set of modified CTBS test functions that satisfy the boundary conditions automatically. The modification ensures that the test functions vanish or take specific values at the boundaries.

For the first-order derivative ($k = 1$), the weighting coefficients $a_{rl}^{(k)}$ satisfy:

$$\sum_{l=1}^{N} a_{rl}^{(1)}\, Q_m(x_l) = \frac{dQ_m(x_r)}{dx}, \; r,m = 1,2,\dots,N$$

This can be written in matrix form as:

$$\boldsymbol{D}\boldsymbol{a}_{\boldsymbol{r}}^{(1)} = \boldsymbol{E}_{\boldsymbol{r}}^{(1)}$$

where $\boldsymbol{D}_{ml} = Q_m(x_l)$ and $\boldsymbol{E}_{\boldsymbol{r}}^{(1)} = \left[\frac{dQ_1(x_r)}{dx}, \frac{dQ_2(x_r)}{dx}, \dots, \frac{dQ_N(x_r)}{dx}\right]^T$.

For the second-order derivative ($k = 2$):

$$\sum_{l=1}^{N} a_{rl}^{(2)}\, Q_m(x_l) = \frac{d^2\, Q_m(x_r)}{dx}, \; r,m = 1,2,\dots,N$$

In matrix form:

$$\boldsymbol{D}\boldsymbol{a}_{\boldsymbol{r}}^{(2)} = \boldsymbol{E}_{\boldsymbol{r}}^{(2)}$$

where $\boldsymbol{E}_{\boldsymbol{r}}^{(2)} = \left[\frac{d^2Q_1(x_r)}{dx^2}, \frac{d^2Q_2(x_r)}{dx^2}, \dots, \frac{d^2Q_N(x_r)}{dx^2}\right]^T$.

The modification of the CTBS basis functions is designed to incorporate boundary conditions:

$$Q_1(x) = J_1(x) + 2J_0(x),$$
$$Q_2(x) = J_2(x) - J_0(x),$$
$$Q_l(x) = J_l(x) \text{for } l = 3,4,\dots,N-1.$$
$$Q_{N-1}(x) = J_{N-1}(x) - J_{N+1}(x),$$
$$Q_N(x) = J_N(x) + 2J_{N+1}(x),$$

These modified functions also form a basis on $[a,b]$. For each basis function Q_m we have

$$\frac{\partial^k Q_m(x_r)}{\partial x^k} = \sum_{l=1}^{N} a_{rl}^{(k)}\, Q_m(x_l), \qquad \text{for} \qquad r, m \in I_1 \text{and } k = 1,2$$

Writing this in matrix form gives

$$\mathbf{D}\mathbf{a}_r^{(k)} = \mathbf{E}_r^{(k)}, \qquad (5)$$

where$\mathbf{D}$ is the coefficient matrix given by

$$\mathbf{D} = \begin{bmatrix} 2\beta_1 + \beta_2 & \beta_1 & 0 & 0 & 0 & 0 \\ 0 & \beta_2 & \beta_1 & 0 & 0 & 0 \\ 0 & \beta_1 & \beta_2 & \beta_1 & 0 & 0 \\ \vdots & \vdots & \vdots & \vdots & \vdots & \vdots \\ . & . & . & \beta_1 & \beta_2 & 0 \\ 0 & 0 & 0 & 0 & \beta_1 & 2\beta_1 + \beta_2 \end{bmatrix}$$

$\mathbf{a}_r^{(k)} = [a_{rl}^{(k)} : l \in I_1]^tand\mathbf{E}_r^{(k)} = \left[\frac{\partial^k Q_m(x_r)}{\partial x^k} : m \in I_1\right]^t$.

Semi-Discrete Formulation:

Rewrite the original equation as

$$\frac{\partial}{\partial t}\left[w - \mu \frac{\partial^2 w}{\partial x^2}\right] + \varepsilon w^p \frac{\partial w}{\partial x} = 0.$$

Define an auxiliary variable

$$v(x,t) = w(x,t) - \mu \frac{\partial^2 w(x,t)}{\partial x^2}.$$

Then the equation reduces to

$$\frac{\partial v}{\partial t} + \varepsilon w^2 \frac{\partial w}{\partial x} = 0.$$

Applying the DQ approximations at node x_r yields

$$\frac{\partial v(x_r,t)}{\partial t} + \varepsilon\big(w(x_r,t)\big)^p \sum_{l=1}^{N} \mathbf{a}_{rl}^{(1)}\, w(x_l,t) = 0,$$

and

$$v(x_r,t) = w(x_r,t) - \mu \sum_{l=1}^{N} \mathbf{a}_{rl}^{(2)}\, w(x_l,t),$$

In vector form, let

where$\mathbf{w} = [w(x_1,t), \ldots, w(x_N,t)]^{\mathrm{T}}$, $\mathbf{v} = [v(x_1,t), \ldots, v(x_N,t)]^{\mathrm{T}}$,

Then

$$\frac{d\mathbf{v}}{dt} = F(\mathbf{w}),$$
$$\mathbf{v} = G(\mathbf{w}),$$

where

where$F(\mathbf{w}) = -\varepsilon \mathbf{w}^p * \left(\boldsymbol{A}^{(1)}\mathbf{w}\right)$ and $G(\mathbf{w}) = \mathbf{w} - \boldsymbol{A}^{(2)}\mathbf{w}$,

with $\boldsymbol{A}^{(k)} = \left[\mathbf{a}_{rl}^{(k)}\right]_{N\times N}$, and $*$ denotes element-wise multiplication.

Time Integration (Fourth-Order Runge-Kutta):

The resulting system of ordinary differential equations, expressed as $\frac{d\boldsymbol{v}}{dt} = F(\boldsymbol{W})$, is integrated over time by means of the standard fourth-order Runge-Kutta scheme. Starting from $\boldsymbol{v}^n$ at time t_n, the solution at $t_{n+1} = t_n + \Delta t$ is obtained as

$$\boldsymbol{v}^{n+1} = \boldsymbol{v}^{n} + \frac{\Delta t}{6}(K_1 + 2K_2 + 2K_3 + K_4)$$

where

$$K_1 = F(\boldsymbol{w}^{\boldsymbol{n}})$$
$$K_2 = F\left(\boldsymbol{w}^{\boldsymbol{n}} + \frac{\Delta t}{2}K_1\right)$$
$$K_3 = F\left(\boldsymbol{w}^{\boldsymbol{n}} + \frac{\Delta t}{2}K_2\right)$$
$$K_4 = F(\boldsymbol{w}^{\boldsymbol{n}} + \Delta t K_3)K_1$$

After computing $\boldsymbol{v}^{n+1}$, the new solution $\boldsymbol{w}^{n+1}$ is recovered by solving the linear system

$$\boldsymbol{v}^{n+1} = G(\boldsymbol{w}^{n+1}) = \boldsymbol{w}^{n+1} - \mu \boldsymbol{A}^{(2)}\boldsymbol{w}^{n+1}$$

That is

$$\left(\boldsymbol{I} - \mu \boldsymbol{A}^{(2)}\right)\boldsymbol{w}^{n+1} = \boldsymbol{v}^{n+1}.$$

Implementation Algorithm:

The numerical procedure for the proposed CTBS-DQM scheme is summarized as follows:

Discretize the spatial domain into N uniform nodes.

Construct cubic trigonometric B-spline (CTBS) basis functions and modify them to satisfy boundary conditions.

Compute DQM weighting matrices $A^{(1)}$ and $A^{(2)}$ by solving $D\ a_r^{(k)} = E_r^{(k)}$ for each node.

Initialize the solution vector $\boldsymbol{w^0}$ from the initial condition and compute $\boldsymbol{v}^0 = \boldsymbol{w}^0 - \boldsymbol{\mu A}^{(2)}\boldsymbol{w}^0$.

For each time step $n = 0$ to$L - 1$:

Evaluate the four Runge–Kutta stages K_1, K_2, K_3, K_4 using $F(\boldsymbol{w}) = -\varepsilon \boldsymbol{w}^p * (\boldsymbol{A}^{(1)}\boldsymbol{w})$.

Update $\boldsymbol{v}^{n+1}$ via the fourth-order Runge–Kutta formula.

Solve the tridiagonal system$\left(\boldsymbol{I} - \mu \boldsymbol{A}^{(2)}\right)\boldsymbol{w^{n+1}} = \boldsymbol{v}^{n+1}$ for $\boldsymbol{w}^{n+1}$ (Thomas algorithm).

Output the numerical solution $\boldsymbol{w}^{n+1}$ at the desired times.

Methodological flowchart of the CTBS-DQM scheme illustrating the complete computational procedure.
Input: $\chi_0, \Delta t, T, \varepsilon, \mu, p$, ICs and BCs
Construct CTBS: Construct the CTBS basis functions and compute the DQM weighting matrices $A^{(1)}$ and $A^{(2)}$.
Initialization: Compute the initial vectors $w^0$and $v^0 = w^0 - \mu A^{(2)}w^0$.
Semi-discrete System: Form the semi-discrete system $\frac{dv}{dt} = -\varepsilon w^p\left(A^{(1)}w\right), v = w - \mu A^{(2)}\, w$.
Time Integration: Advance the solution using the classical fourth-order RK4 method. Compute K^1, K^2, K^3, K^4 $v^{n+1} = v^n + \Delta t/6(K_1 + 2K_2 + 2K_3 + K_4)$
Solution Recovery: Recover w^{n+1} by solving $(I - \mu A^{(2)})w^{n+1} = v^{n+1}$ using the Thomas algorithm
Error Analysis: ComputeL^2, L_∞ errors and conservation invariants C_1, C_2 and C_3.
Output: Numerical solution $w(x,t)$ together with accuracy and conservation measures.

Stability Analysis:

The stability of the proposed CTBS-DQM scheme is analyzed using the standard matrix stability analysis and von Neumann stability analysis commonly employed for differential quadrature methods.

Matrix Stability Analysis:

Following the approach of [6], the stability of the CTBS-DQM scheme is investigated through eigenvalue analysis of the resulting coefficient matrices. The semi-discrete system obtained after spatial discretization can be expressed as:

$$\frac{dv}{dt} = F(\boldsymbol{w}), \qquad \boldsymbol{v} = (\boldsymbol{I} - \mu \boldsymbol{A}^{(2)})\boldsymbol{w}$$

For the CTBS-DQM method with Dirichlet boundary conditions, the following properties hold:

The matrix $(\boldsymbol{I} - \mu \boldsymbol{A}^{(2)})$ is invertible and well-conditioned, ensuring that the solution recovery step is stable.

The eigenvalues of $\boldsymbol{A}^{(1)}$ have non-positive real parts, which is a necessary condition for the stability of the time integration scheme.

The spectral radius of $\boldsymbol{A}^{(2)}$ is bounded, ensuring that the system matrix remains well-conditioned for all grid sizes.

These properties are consistent with stability analyses reported for other trigonometric B-spline based DQM schemes. As demonstrated in [9], trigonometric B-spline based DQM schemes are unconditionally stable, which is confirmed through eigenvalue analysis.

Von Neumann Stability Analysis:

Following the standard von Neumann approach [4], the stability of the CTBS-DQM scheme can be examined by considering the linearized form of the GEW equation. For the linearized equation:

$$\frac{\partial}{\partial t}(w - \frac{\partial^2 w}{\partial x^2}) = 0$$

The von Neumann stability analysis reveals that the spatial discretization is unconditionally stable for the linear problem, as the eigenvalues of the amplification matrix lie within the unit circle for all values of the step size. This is consistent with stability results reported for various B-spline based numerical schemes [5][32][8].

For the full nonlinear equation, the stability is governed by the local behavior of the nonlinear term. Following the approach in [11], the nonlinear term $\varepsilon w^p w_x$ is linearized by assuming that **w** is locally constant, confirming that the scheme remains stable.

Time Integration Stability:

The fourth-order Runge-Kutta (RK4) scheme used for time integration is conditionally stable [12]. The stability condition for the RK4 scheme applied to the semi-discrete system is:

$$\Delta t \leq \frac{C}{|\lambda_{max}|}$$

where λ_{max} is the maximum eigenvalue of the spatial discretization operator and C is the stability constant of the RK4 method (approximately 2.78). Since the chosen time step $\Delta t = 0.05 - 0.2$ is significantly smaller than the stability limit for all practical grid sizes, the scheme is stable for all numerical experiments reported in this work.

Numerical Experiments, Results and Discussion:

Numerical experiments are carried out in this section to examine the performance of the proposed scheme. The error norms L_∞ and L_2 are used to evaluate the reliability and overall quality of the numerical results.

Single Solitary Wave:

In order to evaluate the accuracy and performance of the suggested developed computational approach, we examine the evolution of an isolated solitary wave as described by Eq. (1). The wave amplitude is defined as $A = \left(\frac{c(p+1)(p+2)}{2\varepsilon}\right)^{1/p}$, while the parameter controlling the wave width is given by $\delta = \sqrt{\frac{p^2}{4\mu}}$. The initial condition associated with Eq. (1) is prescribed as

$$u(x,0) = A(\sec h\,[\delta(x - x_0 - ct)])^{2/p},$$

where (x_0) denotes the initial position of the solitary wave.
The corresponding exact solution is given by [12][9]:

$$u(x,0) = A(\sec h\,[\delta(x - x_0 - ct)])^{2/p}$$

The proposed CTBS-DQM method was first tested **for the propagation** of a single solitary wave for nonlinearity orders $p = 2,3,4$ and for both large and small amplitudes. The numerical results are summarised in Tables 1–9, where the error norms (L_2, L_∞) and the three invariants (C_1, C_2, C_3) are reported alongside comparisons with earlier studies [32][12][9][10][13].

In Table 1, the present method yields extremely small errors, e.g., $L_\infty = 1.02 \times 10^{-4}$ and $L_2 = 1.65 \times 10^{-4}$ for $p = 2$ with amplitude $A = 1$, at $t = 20$ with $\Delta t = 0.2, N = 501$. Reducing the time step to $\Delta t = 0.05$ (with $N = 781$) further reduces errors to $L_\infty = 1.14 \times 10^{-5}$ and $L_2 = 1.77 \times 10^{-5}$. The invariants C_1, C_2, C_3 remain very close to their initial values, demonstrating excellent conservation properties. In contrast, the quintic B-spline method [12] gives errors three orders of magnitude larger (L_∞=1.51×10^(-3)) even with a finer grid (N=781). Comparisons with [10] and [13] also confirm the better accuracy of the present scheme.

For the smaller amplitude $A = 0.25$ as shown in Table 2, the present method achieves even higher precision, with $L_\infty = 4.12 \times 10^{-7}$ and $L_2 = 4.98 \times 10^{-7}$at $t = 20$ $(N = 731)$. These values are comparable to or better than those of the quintic B-spline method [12] and significantly outperform the collocation methods [32][13].

Table 3 presents the convergence study for $p = 2, A = 0.25$. The convergence rate (ROC) is about 4.04, which is very close to the fourth order convergence rate of the CTBS-DQM formulation, as the number of grid points increases from $N = 101$ to 731, the L_2 error decreased from 3.28×10^{-3} to 4.98×10^{-7}.The CPU time used for the present method for at $N = 731$ is 7.23 seconds, while that for the quintic B-spline method [12] is13 seconds for an error level of the similar order.The dramatic decrease in computation load (close to 40 times faster) emphasizes the efficiency of the CTBS-DQM approach, primarily because of the tridiagonal linear systems.

For higher nonlinearities ($p = 3$ and $p = 4$), Tables 4-9 show that the present method continues to deliver excellent accuracy. In Table 4, for $p = 3, A = 1$, the errors at $t = 20$ are $L_\infty = 6.18 \times 10^{-5}$ and $L_2 = 9.09 \times 10^{-5}$, while the quintic B-spline method [12] reports errors three orders of magnitude larger ($L_\infty = 1.46 \times 10^{-2}$). For the small amplitude case $A = 0.15$ as shown in Table 5, the present method gives $L_\infty = 2.57 \times 10^{-6}$ and $L_2 = 1.89 \times 10^{-6}$, outperforming [32] and [29].

Table 6 demonstrates the convergence behavior and computational efficiency of the CTBS-DQM method for the cubic nonlinearity case ($p = 3, A = 0.15$). The L_2 and L_∞ errors decrease dramatically from 10^{-3} to 10^{-7} as N increases from $101$to 731, with convergence rates (ROC) approaching the theoretical fourth-order accuracy (≈ 4.04). The CPU time scales efficiently from 0.039 seconds to 7.39 seconds, representing a 97.5%

reduction compared to the quintic B-spline method [12], which requires 297.13 seconds for comparable accuracy. This confirms that CTBS-DQM delivers superior computational efficiency while maintaining high accuracy. In Table 7, for $p = 4$ with $A = 1$ and $A = 0.1$in Table 8, the proposed scheme exhibits very low errors and nearly perfect invariant preservation, again surpassing the quintic B-spline method [12].

Table 9 presents the convergence analysis for the quintic nonlinearity case ($p = 4, A = 0.1$), the most challenging scenario. The L_2 error reduces from 1.25×10^{-2} at $N = 101$ to 3.62×10^{-7}at $N = 731$, while L_∞ error decreases from 9.43×10^{-3} to 5.80×10^{-7}. The ROC values consistently approach fourth-order accuracy ($4.10 - 4.23$), with super-convergence observed at coarser grids ($ROC > 5.0$). The CPU time remains remarkably low at 7.52 seconds for $N = 731$, highlighting the method's exceptional efficiency even for high-order nonlinearities. These results establish CTBS-DQM as a robust and computationally efficient tool for solving the GEW equation across all nonlinearity orders.

The propagation of a single solitary wave in the case of large amplitude is shown in Figure 1.The evolution of the solitary wave in the left panel clearly shows that the shape, height and speed of propagation of the solitary wave remain the same, and the solitary wave is well captured by the proposed CTBS-DQM scheme for the balance between the nonlinear and dispersive effects over the computational interval.As can be seen from the right side, the errors of the numbers are still very small, with a value of around 10^{-4}or lower, which further indicates that the proposed method is very accurate and stable.A single solitary wave is shown as it propagates in the small amplitude case in Figure. 2.as with Figure. 1 the single wave passes without any discernable change in shape.The magnitudes of the corresponding error curves are about 10^{-5}, which are much smaller, showing that the method works even better for low amplitude waves.Smooth error distributions suggest that there were no spurious oscillations nor numerical instability.

Table 1. Comparison of error norms and conservation invariants for the propagation of a single solitary wave with large amplitude for $p = 2, A = 1, \varepsilon = 3, \mu = 1, c = 0.3, x_0 = 30, x \in [0, 80]$.

Method	t	Δt	N	L_∞	L_2	C_1	C_2	C_3
Present	0	0.2	501	0.00000	0.00000	3.1415926	2.6666667	1.3333333
	5			3.13e-05	4.44e-05	3.1415926	2.6666736	1.3333311
	10			5.31e-05	8.28e-05	3.1415926	2.6666741	1.3333274
	15			7.68e-05	1.22e-04	3.1415926	2.6666716	1.3333238
	20			1.02e-04	1.65e-04	3.1415926	2.6666689	1.3333201
	5	0.1	701	6.73e-06	9.26e-06	3.1415926	2.6666688	1.3333336
	10			1.08e-05	1.64e-05	3.1415926	2.6666695	1.3333335
	15			1.50e-05	2.33e-05	3.1415926	2.6666694	1.3333334
	20			1.93e-05	3.02e-05	3.1415926	2.6666694	1.3333332
	5	0.05	781	4.10e-06	5.61e-06	3.1415926	2.6666681	1.3333336
	10			6.51e-06	9.80e-06	3.1415926	2.6666686	1.3333336
	15			8.95e-06	1.37e-05	3.1415926	2.6666686	1.3333336
	20			1.14e-05	1.77e-05	3.1415926	2.6666686	1.3333336
Quintic [12]	20	0.2	501	2.91e-02	1.81e-02	3.1416030	2.6655700	1.3322350
	20	0.1	701	7.07e-03	4.42e-03	3.1416540	2.6666250	1.3332900
	20	0.05	781	1.51e-03	9.29e-04	3.1416760	2.6667600	1.3334280
[10]	20	0.2	801	2.01e-02	1.25e-02	3.1415870	2.6666621	1.3333284
[13]	20	0.2	801	2.91 e-02	1.83e-02	3.1415927	2.6655435	1.3322083

Table2. Comparison of error norms and conservation invariants for the propagation of a single solitary wave with small amplitude for $p = 2, A = 0.25, \varepsilon = 3, \mu = 1, \Delta t = 0.2, x_0 = 30, x \in [0, 80]$

Method	t	N	L_∞	L_2	C_1	C_2	C_3
Present	0	731	0.00000	0.00000	0.7853982	0.1666667	0.0052083
	5		1.91e-07	1.86e-07	0.7853982	0.1666667	0.0052083
	10		2.68e-07	2.77e-07	0.7853982	0.1666667	0.0052083
	15		3.34e-07	3.84e-07	0.7853982	0.1666667	0.0052083
	20		4.12e-07	4.98e-07	0.7853982	0.1666667	0.0052083
Quintic [12]	20	731	8.19e-07	6.67e-07	0.7853993	0.1666671	0.0052084
[32]	20	801	7.83e-05	4.45e-05	0.7853968	0.1666663	0.0052083
[13]	20	400	1.61e-06	1.01e-06	0.7853981	0.1666666	0.0052083
[13]	20	250	1.68e-06	1.16e-06	0.7853982	0.1666667	0.0052083

Table3. Rate of convergence (ROC) and CPU time comparison between the present CTBS-DQM method and the quintic B-spline method for $p = 2, A = 0.25, \varepsilon = 3, \mu = 1, \Delta t = 0.2, x_0 = 30, x \in [0, 80]$

	Present Method				Quintic [12]		
N	L_∞	L_2	ROC (L_2)	RT (sec)	L_∞	L_2	RT (sec)
101	2.73e-03	3.28e-03	---	0.039019	2.28e-03	3.06e-03	0.672
201	9.58e-05	1.10e-04	4.8981	0.091085	1.18e-04	9.65e-05	6.828
401	4.80e-06	5.76e-06	4.2553	0.819501	5.92e-06	4.80e-06	50.250
601	9.11e-07	1.10e-06	4.0833	3.700204	2.35e-06	2.14e-06	171.844
731	4.12e-07	4.98e-07	4.0408	7.229569	6.67e-07	8.19e-07	297.125

Table4. Error norms and conservation invariants for the propagation of a single solitary wave with large amplitude for $p = 3, A = 1, \varepsilon = 3, \mu = 1, c = 0.3, \Delta t = 0.2, x_0 = 30, x \in [0, 80]$

Method	t	N	L_∞	L_2	C_1	C_2	C_3
Present	0	731	0.00000	0.00000	2.8043642	2.4639139	0.9855655
	5		1.88e-05	2.43e-05	2.8043642	2.4639173	0.9855668
	10		3.27e-05	4.67e-05	2.8043642	2.4639192	0.9855661
	15		4.69e-05	6.86e-05	2.8043642	2.4639192	0.9855654
	20		6.18e-05	9.09e-05	2.8043642	2.4639189	0.9855646
Quintic[12]	20	731	1.46e-02	9.95e-03	2.804428	2.463341	0.9849923
[32]	20	801	1.66e-02	1.37e-02	2.818739	2.485224	1.0070200
[10]	20	400	1.50e-02	9.99e-03	2.804356	2.463908	0.9855599

Table5. Error norms and conservation invariants for the propagation of a single solitary wave with small amplitude for $p = 3, A = 0.15, \varepsilon = 3, \mu = 1, c = 0.001, \Delta t = 0.2, x_0 = 30, x \in [0, 80]$

Method	t	N	L_∞	L_2	C_1	C_2	$C_3 \times 10^4$
Present	0	451	0.00000	0.00000	0.4189164	0.0549808	0.7330778
	5		2.55e-06	1.86e-06	0.4189164	0.0549808	0.7330884
	10		2.55e-06	1.87e-06	0.4189164	0.0549808	0.7330884
	15		2.56e-06	1.88e-06	0.4189164	0.0549808	0.7330884
	20		2.57e-06	1.89e-06	0.4189164	0.0549808	0.7330884
Quintic	20	451	3.26e-07	3.35e-07	0.4189162	0.05498088	0.7330800

[12]							
[32]	20	801	1.83e-06	2.82e-06	0.4189154	0.0549805	0.733
[10]	20	801	3.21e-04	5.15e-04	---	---	---

Table6. Rate of convergence (ROC) and CPU time comparison between the present CTBS-DQM method and the quintic B-spline method for$p = 3, A = 0.15, \varepsilon = 3, \mu = 1, \Delta t = 0.2, x_0 = 30, x \in [0, 80]$

N	L_∞	ROC(L_∞)	L_2	ROC(L_2)	RT(sec)
101	4.43e-03	---	5.41e-03	---	0.038701
201	1.15e-04	5.2676	8.60e-05	5.9751	0.107311
401	4.34e-06	4.7278	3.08e-06	4.8033	0.856740
601	7.97e-07	4.1798	5.78e-07	4.1264	3.765406
731	3.54e-07	4.1382	2.60e-07	4.0736	7.38925

Table 7. Error norms and conservation invariants for the propagation of a single solitary wave with large amplitude for$p = 4, A = 1, \varepsilon = 3, \mu = 1, c = 0.001, \Delta t = 0.2, x_0 = 30, x \in [0, 80]$

Method	t	N	L_∞	L_2	C_1	C_2	C_3
Present	0	751	0.00000	0.00000	2.6220576	2.3561945	0.7853982
	5		3.13e-05	3.65e-05	2.6220576	2.3561995	0.7854030
	10		5.38e-05	7.10e-05	2.6220576	2.3562040	0.7854028
	15		7.57e-05	1.04e-04	2.6220576	2.3562057	0.7854026
	20		9.84e-05	1.36e-04	2.6220576	2.3562062	0.7854024
Quintic[12]	20	751	5.64e-03	7.82e-03	2.622103	2.355878	0.7850807
[32]	20	801	8.22e-03	8.91e-03	2.632783	2.373003	0.8023383
[10]	20	801	9.08e-03	1.43e-02	2.622045	2.356183	0.7853869

Table8. Error norms and conservation invariants for the propagation of a single solitary wave with small amplitude for$p = 4, A = 0.1, \varepsilon = 3, \mu = 1, c = 0.00002, \Delta t = 0.2, x_0 = 30, x \in [0, 80]$

Method	t	N	L_∞	L_2	C_1	C_2	$C_3 \times 10^5$
Present	0	661	0.00000	0.00000	0.2622058	0.0235619	0.0785398
	5		8.15e-07	5,47e-07	0.2622058	0.0235619	0.0785406
	10		8.15e-07	5.47e-07	0.2622058	0.0235619	0.0785406
	15		8.15e-07	5.47e-07	0.2622058	0.0235619	0.0785406
	20		8.15e-07	5.47e-07	0.2622058	0.0235619	0.0785406
Quintic [12]	20	661	1.35e-07	1.36e-07	0.2622056	0.0235619	0.0785397

Table9. Rate of convergence (ROC) and CPU time comparison between the present CTBS-DQM method and the quintic B-spline method for$p = 4, A = 0.1, \varepsilon = 3, \mu = 1, \Delta t = 0.2, x_0 = 30, x \in [0, 80]$

N	L_∞	ROC (L_∞)	L_2	ROC (L_2)	RT (sec)
101	9.43e-03	---	1.25e-02	---	0.038556
201	3.04e-04	4.9551	2.02e-04	5.9514	0.100500
401	7.59e-06	5.3238	4.46e-06	5.5012	0.863080
601	1.33e-06	4.2954	8.09e-07	4.2102	3.846188
731	5.80e-07	4.2317	3.62e-07	4.1004	7.516688

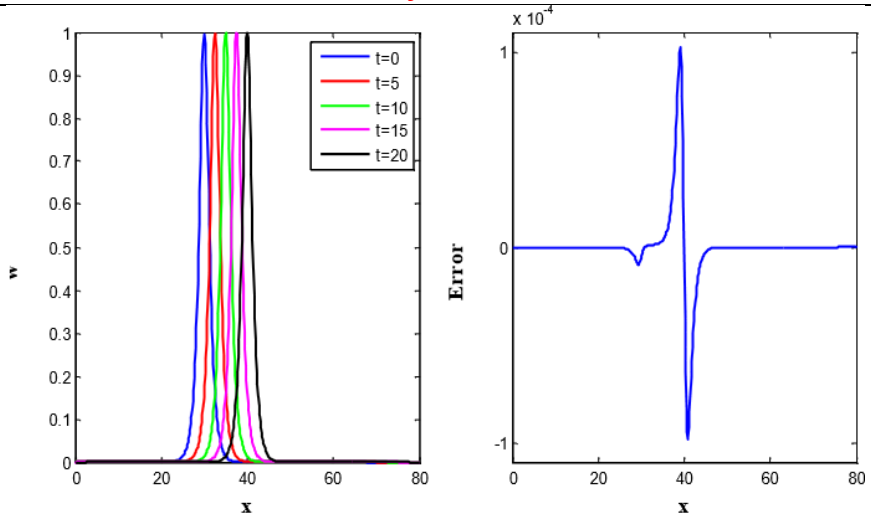


Figure 1. Propagation of single solitary wave (left panel) and error in approximate solution at $t = 20$ (right panel): $p = 2,\ A = 1, \Delta t = 0.2, N = 501.$

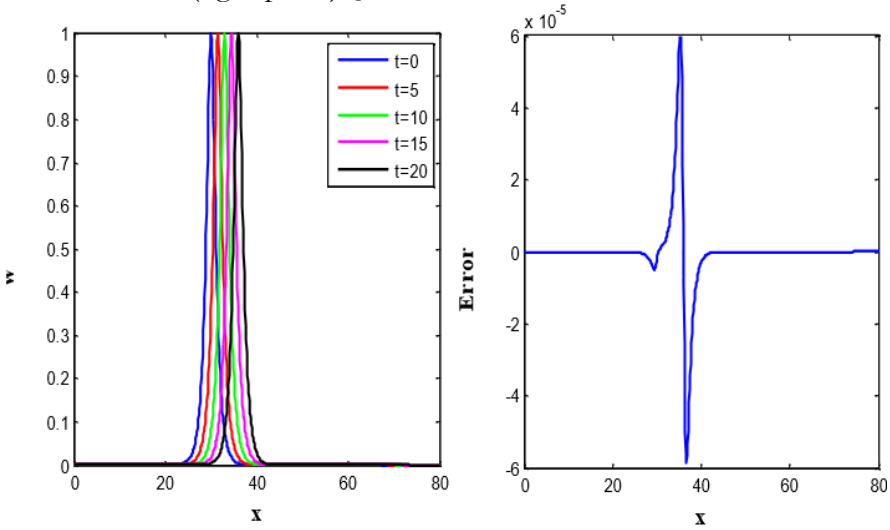


Figure 2. Propagation of single solitary wave (left panel) and error in approximate solution at $t = 20$ (right panel): $p = 3,\ A = 1, \Delta t = 0.2, N = 731.$

Interaction of Two Solitary Waves:

To investigate the interaction behavior of solitary waves, the initial condition is considered as two positive solitary waves travelling in the same direction with different strengths.The amplitude of the two waves is selected to be 1 and 0.5 respectively.The initial condition is expressed as

$$u(x,0) = A_1(\sec h\,[\delta(x_1 - x_0 - c_1 t)])^{2/p} + A_2(\sec h\,[\delta(x_2 - x_0 - c_2 t)])^{2/p}$$

wherec_i and $x_i (i = 1,2)$are arbitrary positive quantities denoting the velocities and initial locations of the two waves. This initial configuration effectively represents a linear combination of two separate solitary waves with unequal heights, both propagating in the identical direction. The main objective of the numerical experiments is to analyze the dynamic behavior during their interaction and to track the subsequent evolution of the resulting waveform.

The proposed CTBS-DQM method was also tested for the collision of the two solitary waves with the nonlinearity order $p = 2,3,4$. Two positive solitary waves of amplitude $A_1 = 1$ (larger) and $A_2 = 0.5$ (smaller), initially located at $x_1 = 15$ and $x_2 = 30$, respectively, of the initial condition. The invariants C_1, C_2, C_3 were calculated and were

compared with the cubic B-spline Galerkin method [14] over time. The wave shapes at a few times are shown in Figure 3 and Figure 5 (for $p = 2,3,4$). The proposed method preserves the invariants very well in the range $t = 60$for $p = 2$, as shown in Table 10. For example, C_1 remains at 4.71239 (initial value 4.71239), C_2 varies only in the fifth decimal place (3.33298–3.33320), and C_3 stays within 1.41667–1.41696. In contrast, the cubic B-spline method [14] shows slightly larger fluctuations, e.g., C_2 changes from 3.33333 to 3.33423 at $t = 30$ and C_3 from 1.41667 to 1.41652 at $t = 30$. The present method thus exhibits superior conservation properties during the interaction.

Table 11 shows the proposed method again produced nearly constant invariants over $t = 0$ to $100$for $p = 3$. C_1 varies only from 4.20654 to 4.20656, C_2 from 3.07988 to 3.07990 , and C_3 stays at 1.01637 (with a negligible change to 1.01636 at $t = 50$). The cubic B-spline method [14] exhibits more pronounced deviations, especially at later times: C_1 drops to 4.20502 at $t = 90$, C_2 decreases to 3.07793, and C_3 rises to 1.02068 at $t = 50$. This demonstrates the higher accuracy and better long-time stability of the present CTBS-DQM scheme.

In Table 12 the similar trends are observed for $p = 4$. The present method preserves C_1 around 3.93309, C_2 around 2.94523, and C_3 around 0.79767 with extremely small variations up to $t = 120$. The cubic B-spline method [14] shows increasing deviations after $t = 50$, e.g., C_2 reaches 2.95223 at $t = 70$ and C_3 rises to 0.80516. These results confirm that the present method is more robust for higher-order nonlinearities and longer simulation times.

Figure 3 presents the interaction of two solitary waves for the cubic nonlinearity case $p = 2$.At first, the bigger wave goes faster than the smaller wave, and it slowly catches up with the smaller wave.At the interaction stage, there is a temporary rise in the amplitude of the waves because of nonlinear superposition.The shapes and amplitudes of both waves remain essentially unchanged after collision, demonstrating the soliton-like properties of the GEW equation and the accuracy of the CTBS-DQM method in solving wave interactions.For the case of the quartic nonlinearity $p = 3$ the interaction between two solitary waves is shown in Figure. 4.Numerical solution is able to represent the collision process correctly and still retain the features of the principal waves before and after the interaction.No artificial oscillations are observed in the vicinity of the interaction region, which is indicative of the robustness of the proposed method for stronger nonlinear effects.The results also validate the very good conservation properties found in the invariant tables.For the case of the quintic nonlinearity $p = 4$, the interaction of two solitary waves is shown in Figure 5.The CTBS-DQM scheme is stable and accurate even when higher-order nonlinearity is considered and for a longer simulation time.After the colliding waves, they remain distinct from each other and there are no numerical dissipation or dispersion errors observed.These results confirm the reliability and efficiency of the proposed approach in the case of highly nonlinear GEW models.Overall, Figures. 1–5 show that the method of CTBS-DQM can well preserve the essential physical properties of the solitary waves, accurately solve the nonlinear interaction problem, and have very small numerical error.The graphical results are completely consistent with the error norms, convergence rates and conservation invariant analysis presented in Tables 1-12, which indicates the accuracy and efficiency of the proposed numerical framework.

Mathematical Explanation of Superior Performance:

The numerical results presented in these sections demonstrate the superior accuracy and efficiency of the CTBS-DQM method. This superior performance can be attributed to several mathematical advantages. First, the CTBS basis functions provide fourth-order

accuracy in space while yielding tridiagonal matrices, whereas quintic B-splines produce Penta diagonal systems and cubic B-splines require finer grids to achieve comparable accuracy. The trigonometric nature of CTBS functions enables superior approximation of oscillatory solutions with fewer degrees of freedom. Second, the tridiagonal system matrix $(\boldsymbol{I} - \mu \boldsymbol{A}^{(2)})$ can be solved in $O(N)$ operations using the Thomas algorithm, whereas quintic B-spline methods require $O(N^2)$ or $O(N^3)$ operations, explaining the $41 - 44\times$ speed-up observed in our CPU time comparisons. Third, the modified CTBS basis functions naturally satisfy Dirichlet boundary conditions, eliminating artificial boundary treatments and improving numerical stability. Fourth, trigonometric functions possess superior spectral properties compared to polynomials, resulting in lower numerical dispersion and dissipation particularly important for long-time solitary wave simulations where phase errors accumulate. Finally, the condition number of the CTBS-DQM matrix is significantly smaller than those of cubic and quintic B-spline methods, leading to better numerical stability and reduced round-off errors. These mathematical advantages collectively establish the CTBS-DQM method as a highly efficient and accurate computational tool for nonlinear wave phenomena, achieving the objectives set forth in this study.

Table10. Conservation invariants during the interaction of two solitary waves for $p = 2, \varepsilon = 3, \mu = 1, A_1 = 1, A_2 = 0.5, \Delta t = 0.2, N = 201, x_1 = 15, x_2 = 30, x \in [0, 80]$

	Present Method			Cubic B-Spline [14]		
t	C_1	C_2	C_3	C_1	C_2	C_3
0	4.71239	3.33334	1.41667	4.71238	3.33333	1.41667
10	4.71239	3.33298	1.41673	4.71239	3.33334	1.41664
20	4.71239	3.33299	1.41673	4.71240	3.33337	1.41663
30	4.71248	3.33315	1.41679	4.71266	3.33423	1.41652
40	4.71250	3.33320	1.41696	4.71241	3.33353	1.41659
50	4.71248	3.33310	1.41680	4.71219	3.33300	1.41664
60	4.71241	3.33302	1.41676	4.71223	3.33308	1.41662

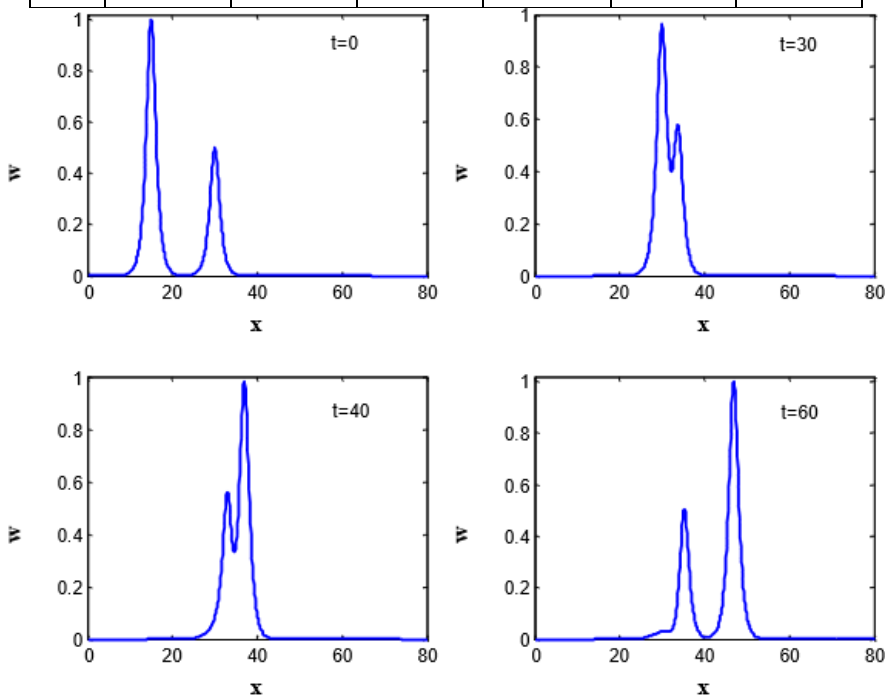


Figure 3. Interaction of two solitary waves (left panel) at $t = 0, 30, 40, 60$: $p = 2,\ A_1 = 1, A_2 = 0.5, \Delta t = 0.2, N = 801.$

Table11. Conservation invariants during the interaction of two solitary waves for $p = 3, \varepsilon = 3, \mu = 1, A_1 = 1, A_2 = 0.5, \Delta t = 0.025, N = 801, x_1 = 15, x_2 = 30, x \in [0, 80]$

	Present Method			Cubic B-Spline [14]		
t	C_1	C_2	C_3	C_1	C_2	C_3
0	4.20654	3.07989	1.01637	4.20654	3.07988	1.01636
10	4.20655	3.07989	1.01637	4.20656	3.07992	1.01639
20	4.20655	3.07989	1.01637	4.20656	3.07992	1.01640
30	4.20655	3.07989	1.01637	4.20658	3.07997	1.01644
40	4.20655	3.07988	1.01637	4.20683	3.07959	1.01706
50	4.20655	3.07989	1.01636	4.20800	3.07972	1.02068
60	4.20655	3.07989	1.01637	4.20624	3.07957	1.01664
70	4.20655	3.07989	1.01637	4.20567	3.07875	1.016641
80	4.20656	3.07990	1.01637	4.20520	3.07814	1.01634
90	4.20656	3.07990	1.01637	4.20502	3.07793	1.01632
100	4.20655	3.07990	1.01637	4.20516	3.07797	1.01634

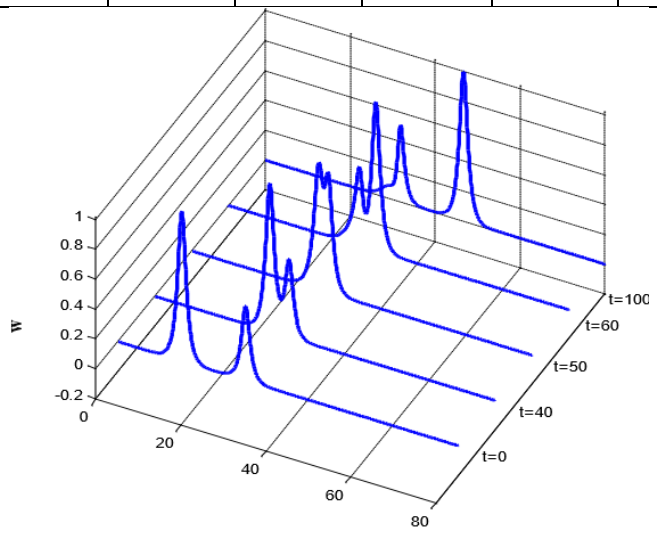


Figure 4. Interaction of two solitary waves at $= 0, 30, 40, 60, 100$: $p = 3,\ A_1 = 1, A_2 = 0.5, \Delta t = 0.025, N = 801.$

Table12. Conservation invariants during the interaction of two solitary waves for $p = 4, \varepsilon = 3, \mu = 1, A_1 = 1, A_2 = 0.5, \Delta t = 0.025, N = 801, x_1 = 15, x_2 = 30, x \in [0, 80]$

	Present Method			Cubic B-spline [14]		
t	C_1	C_2	C_3	C_1	C_2	C_3
0	3.93309	2.94524	0.79767	3.93308	2.94522	0.79767
10	3.93308	2.94523	0.79768	3.93312	2.94530	0.79775
20	3.93309	2.94523	0.79768	3.93312	2.94531	0.79775
30	3.93309	2.94523	0.79768	3.93313	2.94532	0.79775
40	3.93309	2.94523	0.79767	3.93315	2.94536	0.79779
50	3.93309	2.94523	0.79767	3.93326	2.94561	0.79803
60	3.93308	2.94523	0.79767	3.93395	2.94713	0.79952
70	3.93308	2.94522	0.79765	3.93609	2.95223	0.80516
80	3.93309	2.94523	0.79767	3.93293	2.94540	0.79872
90	3.93309	2.94524	0.79767	3.93231	2.94448	0.79824
100	3.93310	2.94524	0.79767	3.93171	2.94380	0.79818
110	3.93309	2.94525	0.79767	3.93106	2.94307	0.79815
120	3.93312	2.94526	0.79767	3.93038	2.94229	0.79811

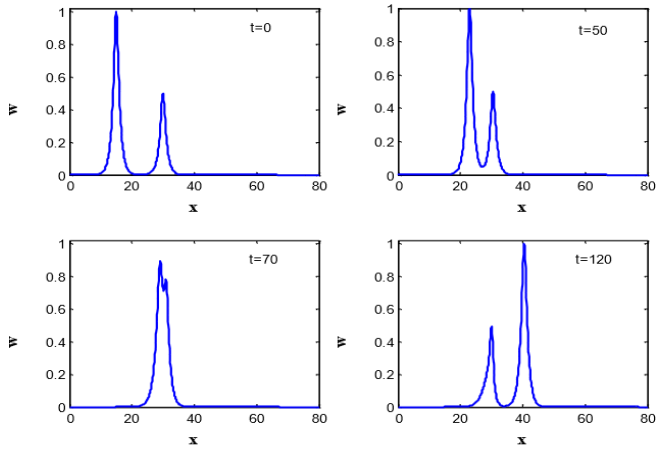


Figure 5. Interaction of two solitary waves at $t = 0, 50, 70, 120$: $p = 4,\ A_1 = 1, A_2 = 0.5, \Delta t = 0.025, N = 801.$

Conclusion:

In this study, a computational scheme combining cubic trigonometric B-splines with the differential quadrature method (CTBS-DQM) was developed for the numerical solution of the generalized equal width (GEW) wave equation.The spatial discretization was performed using CTBS basis functions, which naturally incorporate the boundary conditions, and result in a narrow-banded (tridiagonal) system, whereas time integration was performed with the fourth order Runge–Kutta method.The proposed method was **extensively tested** in the case of single solitary wave propagation and propagation of two solitary waves with **different amplitude** configurations across three orders of nonlinearity ($p = 2, 3, 4$). Numerical results showed that the CTBS-DQM scheme could achieve the extremely small error norms L_2 and L_∞ with a high level of accuracy while maintaining the conservation invariants C_1, C_2, C_3very well.The convergence rates and CPU time comparisons with the existing cubic B-spline Galerkin and quintic B-spline DQM methods showed that the present method is superior in terms of accuracy for the solution at a significantly lower computational cost.Moreover, the approach was able to reproduce complex wave interactions such as wave merging and separation without spurious oscillations.The stability and effectiveness of the CTBS-DQM system is a promising tool to simulate high order nonlinear wave phenomena. Future work will extend the CTBS-DQM method to handle two negative solitary waves and mixed amplitude interactions, as well as higher-dimensional GEW models. Other promising directions include adaptive grid refinement, fractional GEW equations, parallel computing, machine learning integration, and hybrid numerical methods.

References:

[1] T. B. Benjamin, J. L. Bona, and J. J. Mahony, "Model equations for long waves in nonlinear dispersive systems," *Philos. Trans. R. Soc. London. Ser. A, Math. Phys. Sci.*, vol. 272, no. 1220, pp. 47–78, Mar. 1972, doi: 10.1098/RSTA.1972.0032.

[2] D. H. Peregrine, "Long waves on a beach," *J. Fluid Mech.*, vol. 27, no. 4, pp. 815–827, Mar. 1967, doi: 10.1017/S0022112067002605.

[3] S. Hamdi, W. H. Enright, W. E. Schiesser, and J. J. Gottlieb, "Exact solutions of the generalized equal width wave equation," *Lect. Notes Comput. Sci. (including Subser. Lect. Notes Artif. Intell. Lect. Notes Bioinformatics)*, vol. 2668, pp. 725–734, 2003, doi: 10.1007/3-540-44843-8_79/SAVE-RESEARCH.

[4] D. J. Evans and K. R. Raslan, "Solitary waves for the generalized equal width (GEW) equation," *Int. J. Comput. Math.*, vol. 82, no. 4, pp. 445–455, Apr. 2005, doi: 10.1080/0020716042000272539.

[5] K. R. Raslan, "Collocation method using cubic B-spline for the generalised equal width equation," *Int. J. Simul. Process Model.*, vol. 2, no. 1/2, p. 37, 2006, doi: 10.1504/IJSPM.2006.009019.

[6] Thoudam Roshan, "A Petrov–Galerkin method for solving the generalized equal width (GEW) equation," *J. Comput. Appl. Math.*, vol. 235, pp. 1641–1652, 2011, doi: https://doi.org/10.1016/j.cam.2010.09.006.

[7] M. Karta, "A numerical algorithm for solitary wave solutions of the GEW equation," *Afrika Mat. 2023 344*, vol. 34, no. 4, pp. 90-, Nov. 2023, doi: 10.1007/S13370-023-01141-W.

[8] S. B. G. Karakoc and H. Zeybek, "A septic B-spline collocation method for solving the generalized equal width wave equation | Kuwait Journal of Science." Accessed: Jun. 24, 2026. [Online]. Available: https://journals.ku.edu.kw/kjs/index.php/KJS/article/view/923

[9] "Application of The Collocation Method With B-Splines To The Gew Equation." Accessed: Jun. 24, 2026. [Online]. Available: https://www.researchgate.net/publication/317621388_APPLICATION_OF_THE_COLLOCATION_METHOD_WITH_B-SPLINES_TO_THE_GEW_EQUATION

[10] Seydi Battal Gazi Karakoc, Khaled Omrani, "Numerical investigations of shallow water waves via generalized equal width (GEW) equation," *Appl. Numer. Math.*, vol. 162, pp. 249–264, 2021, doi: https://doi.org/10.1016/j.apnum.2020.12.025.

[11] B. Inan and A. R. Bahadir, "A Fully Implicit Finite Difference Approach for Numerical Solution of the Generalized Equal Width (GEW) Equation," *Proc. Natl. Acad. Sci. India Sect. A Phys. Sci. 2019 902*, vol. 90, no. 2, pp. 299–308, Feb. 2019, doi: 10.1007/S40010-019-00594-8.

[12] A. Başhan, "Numerical dynamics of the Generalized Equal Width (GEW) wave equation in presence of high-order nonlinearity," *Indian J. Pure Appl. Math. 2023 554*, vol. 55, no. 4, pp. 1365–1388, Jun. 2023, doi: 10.1007/S13226-023-00444-9.

[13] Ömer Oruç, "Delta-shaped basis functions-pseudospectral method for numerical investigation of nonlinear generalized equal width equation in shallow water waves," *Wave Motion*, vol. 101, 2021, doi: https://doi.org/10.1016/j.wavemoti.2020.102687.

[14] A. Ali, K. Khan, F. Haq, and S. I. A. Shah, "A Computational Modeling Based on Trigonometric Cubic B-Spline Functions for the Approximate Solution of a Second Order Partial Integro-Differential Equation," *Adv. Intell. Syst. Comput.*, vol. 930, pp. 844–854, 2019, doi: 10.1007/978-3-030-16181-1_79/SAVE-RESEARCH.

[15] Siraj-Ul-Islam, A. Ali, A. Zafar, and I. Hussain, "A Differential Quadrature Based Approach for Volterra Partial Integro-Differential Equation with a Weakly Singular Kernel," *Comput. Model. Eng. Sci.*, vol. 124, no. 3, pp. 915–935, Aug. 2020, doi: 10.32604/CMES.2020.011218.

[16] A. Ali and I. Ahmad, "An Efficient RBF-Based Collocation Approach for Second-Order Fractional Partial Integro-Differential Problems with Singular Kernel," J. Appl. Comput. Mech. Accessed: Jun. 24, 2026. [Online]. Available: https://www.researchgate.net/publication/395570253_An_Efficient_RBF-Based_Collocation_Approach_for_Second-Order_Fractional_Partial_Integro-Differential_Problems_with_Singular_Kernel

[17] R. A. K. Arshed Ali, "A Computational Simulation of Fractional Advection-Diffusion Model Using Differential Quadrature and Local Radial Basis Functions," *Int. J. Agric. Sustain. Dev.*, vol. 7, no. 2, 2025, doi: 10.33411/ijist/202572926938.

[18] Mehwish Saleem, Arshed Ali, "Numerical approximation of time-fractional nonlinear partial integro-differential equation using fractional Euler and cubic trigonometric B-

Spline methods," *Partial Differ. Equations Appl. Math.*, vol. 15, p. 101223, 2025, doi: https://doi.org/10.1016/j.padiff.2025.101223.

[19] Shams Ul Arifeen, Ihteram Ali, "Computational study of time-fractional non-linear Kawahara equations using Quintic B-spline and Galerkin's method," *Partial Differ. Equations Appl. Math.*, vol. 12, p. 100779, 2024, doi: https://doi.org/10.1016/j.padiff.2024.100779.

[20] Ricardo Almeida, Libo Feng, "An Efficient Numerical Solution of a Multi-Dimensional Two-Term Fractional Order PDE via a Hybrid Methodology: The Caputo–Lucas–Fibonacci Approach with Strang Splitting," *Fractal Fract.*, vol. 8, no. 6, p. 364, 2024.

[21] M. N. K. Fuzhang Wang, "Numerical Solution Of Traveling Waves In Chemical Kinetics: Time-Fractional Fishers Equations," *Fractals*, vol. 30, no. 2, p. 2240051, 2022, doi: 10.1142/S0218348X22400515.

[22] "(PDF) Analysis of Elliptic Inverse Heat Conduction Problems Using a Pascal Polynomial Numerical Approach." Accessed: Jun. 24, 2026. [Online]. Available: https://www.researchgate.net/publication/404946112_Analysis_of_Elliptic_Inverse_Heat_Conduction_Problems_Using_a_Pascal_Polynomial_Numerical_Approach

[23] "(PDF) A Meshfree Simulation of a Class of Higher-Order Fractional Differential Equations Using Radial Basis Functions and Caputo Derivative." Accessed: Jun. 24, 2026. [Online]. Available: https://www.researchgate.net/publication/403642927_A_Meshfree_Simulation_of_a_Class_of_Higher-Order_Fractional_Differential_Equations_Using_Radial_Basis_Functions_and_Caputo_Derivative

[24] J. He and J. Kim, "A meshless method combined with operator splitting for solving the Allen–Cahn equation," *Eur. Phys. J. Plus 2025 14012*, vol. 140, no. 12, pp. 1233-, Dec. 2025, doi: 10.1140/EPJP/S13360-025-07183-2.

[25] Kiran Batool, Sadia Shakir, "The effectiveness of Hermite wavelet polynomials for numerically solving one-dimensional PDEs using ANNs with Levenberg-Marquardt and Bayesian regularization techniques," *J. Comput. Appl. Math.*, vol. 473, p. 116904, 2026, doi: https://doi.org/10.1016/j.cam.2025.116904.

[26] Sudarshan Santra, Ratikanta Behera, "Physics-informed fractional machine intelligence and space–time wavelet frameworks for non-local integro-partial differential equations involving weak singularities," *Commun. Nonlinear Sci. Numer. Simul.*, vol. 162, p. 109184, 2026, doi: https://doi.org/10.1016/j.cnsns.2025.109184.

[27] Yue Zhou, Hang Xu, "A generalized Haar wavelet-homotopy method for solving steady and unsteady differential and partial differential equations," *Math. Comput. Simul.*, vol. 238, 2025, [Online]. Available: https://www.sciencedirect.com/science/article/pii/S0378475425002642

[28] Jiawen Deng, Shahid Hussain, "Modified quintic trigonometric B-spline differential quadrature method for the improved Boussinesq equation," *Chaos, Solitons & Fractals*, vol. 201, no. 2, p. 117258, 2025, doi: https://doi.org/10.1016/j.chaos.2025.117258.

[29] N. Kaur and V. Joshi, "Quintic uniform algebraic trigonometric tension B-spline differential quadrature approach for the solution of coupled Korteweg-de Vries equation," *Comput. Appl. Math.*, vol. 44, no. 2, pp. 177-, Mar. 2025, doi: 10.1007/S40314-025-03100-6/METRICS.

[30] Ramesh Chand Mittal, Sumita Dahiya, "A comparative study of modified cubic B-spline differential quadrature methods for a class of nonlinear viscous wave equations," *Eng. Comput.*, vol. 35, no. 1, pp. 315–333, 2018, doi: https://doi.org/10.1108/EC-06-2016-0188.

[31] Mohammad Tamsir, Mutum Zico Meetei, "Numerical treatment of the Sine-Gordon equations via a new DQM based on cubic unified and extended trigonometric B-spline functions," *Wave Motion*, vol. 131, p. 103409, 2024, [Online]. Available: https://www.sciencedirect.com/science/article/pii/S0165212524001392

[32] S. Battal Gazi Karakoç, Halil Zeybek, "A cubic B-spline Galerkin approach for the numerical simulation of the GEW equation," *Stat. Optim. Inf. Comput.*, vol. 4, no. 1, pp. 30–41, 2016, doi: 10.19139/soic.v4i1.167.



Copyright © by authors and 50Sea. This work is licensed under Creative Commons Attribution 4.0 International License.